Optimizing Rail Journeys with Simultaneous Improvement in Energy Consumption and Service Quality

Mohammad Hossein Bigharaz[*]

Metro and Railway Group, Transmission and Distribution Division, Monenco Iran Consulting Engineers

ARTICLE INFO	A B S T R A C T
	With rapid development of the state-of-the-art railway transportation systems, requirements in expanding energy resources and better service quality are increased. Competitors in this field will probably focus on how to execute an optimal journey, which not only maximizes the service quality but also takes minimum energy consumption. This article is proposing efficient travel by a train under some predefined constraints in track profile and speed limits. In this context, multi-objective evolutionary techniques including NSGA-II and MOPSO are modified and adapted to accomplish the regarding speed trajectories with two conflict objectives i.e. minimum energy consumption and minimum journey time delay. In order to make the travel more comfortable, some equations are developed and are introduced into the optimization process. Robustness of the solutions is regarded as an additional criterion for proving the efficiency of the planned solutions.

1. Introduction

Population growth, heavy traffics, safety requirements and increasing transportation expenses cause almost all countries to pay more attention in developing their railway transportation systems. Reducing energy consumption and simultaneously maximizing service quality can be considered as two significant issues in railway engineering. Originally, in order to minimize the total energy consumption, railway industries came across two independent procedures: a) improving fabrication technology and b) developing the control methods. Obviously, executing any improvement in fabrication process of current railway systems is accompanied with many commercial expenses [1]. However improving the controlling procedures such as applying efficient driving strategy and looking for an optimal timetable for the current system can be easily achieved and does not impose significant

expenses [2]. In this way, performing optimal speed trajectories on a train system can effectively reduce the energy consumption with minimum cost rather than making changes into the infrastructure. Optimal speed trajectories can be utilized by driver assistant system (DAS) and automatic train operation (ATO) system to modify their journey strategies [3]. Many studies concerning energy minimization approaches are accomplished in railway applications. Yang et al. [4] studied a mathematical model with a predefined path and then used a coasting control strategy with genetic algorithm (GA) method to find optimal trajectories of a train. In order to investigate advanced power management strategies for Diesel multiple unit trains, Lu et al. [5] evaluated the potential of energy saving through independent operation of motors using dynamic programming (DP) method. Based on the control strategies, the accomplished studies in this context can be categorized into two major groups including coasting control and global control. In order to search for the specific points

[*]Corresponding author
Email: Bigharaz.mohammad@monencogroup.com

where optimal speed trajectory is assured, coasting control methods are applicable [6-8]. Applying global control approaches can be accompanied with many difficulties and cause a heavy calculation burden because all available signals need to be used to produce an optimal speed trajectory [9-10]. Lu et al. [11] used DP, ant colony optimization (ACO) and GA methods to create optimal speed trajectories with minimum energy consumption while observing journey time and speed constraints. They demonstrated that DP is capable of producing speed trajectories with better performance but with heavier calculation burden and under some limited quantized inputs. Because of the conflict between energy consumption and journey time delay, using traditional methods for optimizing these objectives simultaneously are difficult or even impossible. Therefore, using evolutionary methods in these problems can potentially lead to acceptable results [12, 13].

In the present research, the train is considered as a plant with a sequence of several modes including motoring, cruising, braking and coasting. A suitable strategy is developed to implement an efficient driving with allocating a dynamic control index which satisfies traveler comfort. The rail path between two stations is divided into n predefined zones and a graph with k×n nodes is considered. The modified versions of two multi-objective evolutionary strategies including NSGA-II and MOPSO are applied to the problem. The final solutions are evaluated by using the Pareto fronts optimization method and are compared based on several criteria including the energy minimization, performance and robustness. The initial work on this topic is reported in [14].

2. Vehicle Modelling

The use of computer simulations in railway engineering goes back to the time when computer techniques started flourishing (i.e. 1970s) [15]. Modelling of rail vehicles' movements were accomplished to compute the distance, time and velocity status of a moving train on a track under speed limits and traction devices' constraints. Based on the Newton's second law of motion, the motion of a vehicle can be expressed as in Equation (1):

$$M_{eff}\ \frac{d^2x}{dt^2} = f_T - R - Mg\sin(\alpha) \qquad (1)$$

where f_T is the traction force (N.m), M_{eff} is the effective mass (kg), R is the train resistance to move forward (N), g is the gravitational force (N), α is the angle of track slop and x is the current train distance (m).

In addition to the stationary components, every vehicle possesses some rotary features that affect the effective mass. Hence, a rotary allowance coefficient is required to increase the accuracy of calculations [16].

$$M_{eff} = M\,(1+\tau) \qquad (2)$$

where τ is the rotary allowance and usually is assumed to be less than 0.2 [16].

In general, the vehicle control inputs are divided into four modes: motoring, coasting, cruising and braking. During motoring mode, which includes full motoring and partial motoring, the train is accelerated and its velocity is raised from the low speed level to the higher amounts. During the cruising mode, velocity is held at a constant level. When train operates in coasting mode, traction motors do not produce any torque, thus the total energy consumed by the traction motors is zero. In practice, the acceleration is influenced by the total resistance and gravitational effects. In this situation, determining the coasting point where, the train enters the coasting mode at that point has an indisputable effect on the total energy consumption [17]. During the braking mode including full and partial braking, the train speed is decreased to reach to a lower speed limit or to stop at the station. Some critical requirements for braking mode exists which consists of assuring that the train speed always remains under certain level and also the train arrives at the station with a zero level of speed. Several methods are introduced to determine the exact point of entering to the braking mode. In some studies, a train is assumed to be located at the destination point and then it moves inversely by an analogous traction force to create a speed trajectory. After that, the resulted trajectory is intersected to the normal train speed trajectory. Obviously, the intersection point will be the exact braking point [18]. Frankly, this method is efficient when the train goes into the braking mode by a constant braking ratio and it does not stand with a varying one. In the present research, a method is proposed which applies a virtual braking process in each moment, once the train enters to a predefined braking area. The proposed method determines the exact braking

point meanwhile it actually meets the efficiency for various braking ratios.

2.1. State Equations and Objective Functions

The state of a train can be expressed as in Equation (3):

$$\begin{bmatrix} \dot{x} \\ \dot{v} \end{bmatrix} = \begin{bmatrix} v \\ \dfrac{1}{M_{eff}}(f(u(t),v(t))-r(v)-G(x,v)) \end{bmatrix} \tag{3}$$

where x, v, and u represent position, velocity and input signal of the train, respectively. r implies the resistance against the train movement which is presented in Equation (4). f is expressed in Equation (5) and is the force that is applied to the train wheels. G is the longitudinal force imposed by tunnels, slopes and curvatures of the track to the train of length L.

$$r(v) = A + B \cdot v + C \cdot v^2 \tag{4}$$

A, B and C are the empirical factors that are related to the Davis train resistance coefficients [19].

$$f(u(t),v(t)) = u(t) \cdot TE^{acc}(t) \tag{5}$$

$TE^{acc}(t)$ is the maximum accessible traction effort that can be expressed as in Equation (6):

$$TE^{acc}(t) = \frac{\mu \cdot P_n}{v(t)} \tag{6}$$

where μ and P_n are friction factor and nominal power of traction motors in the train. The longitudinal force per mass unit can be expressed as in Equation (7):

$$G(x,v) = mg\sin(\alpha(x)) + f_C(R(x)) + f_t(L_t(x),v) \tag{7}$$

where $a(x)$, $R(x)$ and $L_t(x)$ are the slope, the radius of the track curve, and the length of the tunnel along the track, respectively. $f_c(\cdot)$ and $f_t(\cdot)$ are the curvature and tunnel resistances, both are given by the experimental equations. The curvature resistance can be obtained by using the Roeckle experimental Equation (8) [20]:

$$\begin{cases} f_C(R(x)) = \dfrac{6.3}{R(x)-55}m & for \ \ R(x) \geq 300m \\[2mm] f_C(R(x)) = \dfrac{4.91}{R(x)-30}m & for \ \ R(x) < 300m \end{cases} \tag{8}$$

Undoubtedly, trains confront aerodynamic resistance when entering the tunnels. This resistance is related to several factors such as the tunnel shape, the smoothness of tunnel walls, and the exterior surface of the train [20]. The tunnel resistance is defined as follows:

$$f_t(L_t(x,v) = a_t(L_t(x)) \cdot v^2 \tag{9}$$

The multi-objective problem of simultaneous optimization of the train energy consumption and travelling time can be written as a set Φ, including two objective functions.

$$\Phi = (\varphi_1,...,\varphi_n) \ , \ \ n \leq 2 \tag{10}$$

The first objective function, φ_1 is related to energy minimization and the second one φ_2 explores the minimum travelling time.

$$\varphi_1 = \min E \tag{11}$$

$$\varphi_2 = \min T \tag{12}$$

The energy consumed by the train can be calculated as in the following Equation (13):

$$E = \int_{t_0}^{t_f} P(t)dt = \int_{t_0}^{t_f} f(u(t),v(t)) \cdot v(t)dt$$
$$= \int_{t_0}^{t_f} u(t) \cdot TE^{acc}(t) \cdot v(t)dt \tag{13}$$

The travel time of the train equals the sum of the total time durations that is needed to travel over a zone in a track with n zones. This statement is presented in Equation (14).

$$T = \sum_{k=1}^{n} T_k \tag{14}$$

T_k represents the time duration that train spends to pass through the kth zone. Constraints and boundary conditions on the problem are stated as:

$$x(t_0) = x_0 \ \ , \ \ v(t_0) = 0 \tag{15}$$

$$x(t_f) = x_f \ \ , \ \ v(t_f) = 0 \tag{16}$$

$$-1 \leq u \leq 1 \tag{17}$$

$$v \leq v_{max}(x) \tag{18}$$

v_{max} is the maximum allowable speed of the train that is determined by the traffic control or ATP system.

The state switching that is presented in Equation (19), is performed by making a change in the traction power. Either driver or ATO decides on this change. A desired state switching requires applying suitable strategies to determine the proper sequences of the control indexes between the two states.

$$\psi_0 = \{x_0, v_0, t_0\} \xrightarrow{f_T} \psi_1 = \{x_1, v_1, t_1\} \qquad (19)$$

2.2. Graph Construction

In order to represent a certain track with n zones and k candidate speeds for each zone, a $k \times n$ nodes graph is developed. The graph is depicted in Figure 1. In each predefined zone, the target speed must be determined so that the train will be capable to follow this speed. These target speeds are defined in the optimization process.
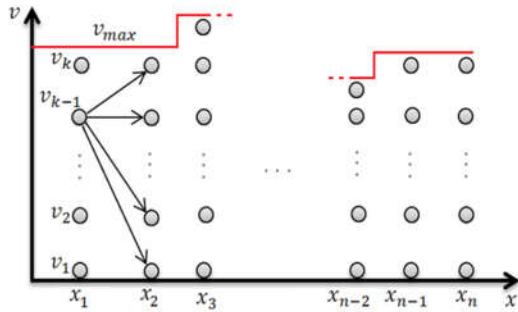

Figure 1. Graph construction

2.3. Driving and Control Index Allocation

In order to generate the speed profile, the track length is divided into n zones, and the speed variables including v_{ei}, v_{ai} and v_{xi} are determined in each zone (Figure 2). For each zone, two sections are considered: the first section contains two speeds of v_{ei} and v_{ai} that are the entrance and candidate speeds, respectively. The second section contains v_{ai} and v_{xi} that are the candidate and exit speeds, respectively. v_{ei} and v_{xi} are determined during the speed profile generation. v_{ai} is obtained by applying the optimization algorithms. If v_{mi} is assumed as the maximum speed corresponding to the ith zone that is defined by ATP system and the track information, the following constraints exist for the ith zone:

$$x(t_0) = x_0 \quad , \quad v(t_0) = 0 \qquad (20)$$

$$x(t_f) = x_f \quad , \quad v(t_f) = 0 \qquad (21)$$

It should be noted that the driver is limited to select only three inputs (i.e. $u \in \{-1, 0, 1\}$) to reach the target speed in each zone. Motoring and braking ratios are determined automatically by the developing strategy that is named the control index k_C at all instances. This is elaborated further on in the next section of this article.
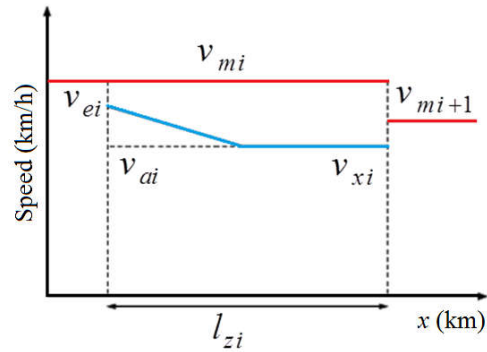

Figure 2. Details of zone i

The ith zone speed trajectory is related to some factors including the decision speed v_{ai}, earth geometry profile, the maximum speed of the current and the next zones and the coasting control capabilities in total zones. The following approach is developed in this research to implement an efficient driving strategy.

a) If $v_{xi} < v_{mi}$, $v_{xi} < v_{mi+1}$:

- If $v_{ai} > v_{ei} \rightarrow$ Motoring

- If $v_{ai} < v_{ei} \rightarrow$ Coasting

- If $v_{ai} = v_{ei} \rightarrow$ Cruising

b) If $v_{xi} > v_{mi+1}$:

- The first case: Coasting. The optimization algorithm evaluates circumstance and situation for switching to the coasting mode intelligently.

- The second case: Braking. If the train cannot reach to the next speed limit by coasting mode, therefore, the train enters to the critical braking distance and it must determine the accurate braking point and its rate to reach favorably to the speed limit.

c) If the train is in the critical distance of the destination $x_{cur} \geq x_{critical}$:

- Throughout this section and regarding to the train's current state, virtual braking processes are performed over some predefined periods. During this procedure, the accurate braking point is assessed.

2.4. Control Index with Traveler Comfort Factors

In some studies that are conducted in the context of optimal train speed trajectory, almost no attention was paid to the traveler comfort criteria. When the train is accelerated or entered

to the braking mode, traveler comfort becomes more significant. Generally, in most railway transportation systems, driver plays a major role in making a desirable and comfortable journey. Therefore, an undesirable performance of the driver can distort the efficient journey. Here, the driver task is limited to only adjusting the mode type (i.e. $u \in \{-1,0,1\}$, where -1 is for braking, 0 is for coasting and 1 is for motoring and cruising). Consequently, the operational control input is defined as in Equation (22):

$$u'(t) = u(t).k_C(t) \qquad (22)$$

where $u(t)$ is selected by the driver and $k_C(t)$ is the control index and is determined in Equations (23-25):

$$\text{mode} = \{\text{motoring}\} \Rightarrow \quad k_c(t) = \frac{v_{ai} - k_m v_{cur}(t)}{v_{ai}} \qquad (23)$$

$$\text{mode} = \{\text{braking}\} \Rightarrow \quad k_c(t) = 1 - \left| \frac{v_{ai} - k_b v_{cur}(t)}{v_{ai}} \right| \qquad (24)$$

$$\text{mode} = \{\text{Cruising}\} \Rightarrow \quad k_c(t) = \frac{r(v) + G(x,v)}{TE^{acc}(t)} \qquad (25)$$

where $v_{cur}(t)$ is the current speed. $k_m, k_b \in [0,1]$ are considered as comfort measures in motoring and braking modes. According to Equation (23), while k_m is approaching to zero, the less comfort criteria is resulted, but the more exact tracking of the speed trajectory is obtained and when it goes to one, the more comfort will be resulted. Figure 3 demonstrates the train acceleration in motoring mode for several k_m values. Undoubtedly, selecting a proper k_m can provide significant improvement in passenger comfort in the motoring mode. Another challenging issue with a great influence on passenger comfort is lack of a satisfactory braking process. However, in the literature, almost all studies consider exactly an inverse motoring traction force for braking process and the effects of a high rise negative acceleration on passenger comfort is neglected. By means of the developed $k_C(t)$, that is presented in Equation (24), the braking mode ratio in each instance is determined with the influencing factor k_b. The resultant $k_C(t)$ can manage the braking mode and causes the train to stop at the station precisely with a smooth decreasing negative acceleration. Figure 4 presents the acceleration curves for different k_b. It is obvious that for $k_b = 0.1$, the negative acceleration during braking mode has a lower extent, and therefore, it causes a better passenger comfort when compared with when $k_b = 1$. According to the earlier expressed content,

determining desirable values for k_b and k_m during the journey is very significant, in a way that, not only the target speed to be tracked properly but also the traveler comfort is satisfied appropriately.

3. Simulation and Results

In this research, two evolutionary multi-objective algorithms, namely NSGA-II and MOPSO are implemented in order to identify the optimal speed trajectories. Optimization is accomplished for two antithetic objectives namely the energy consumption and the time travelling minimization.
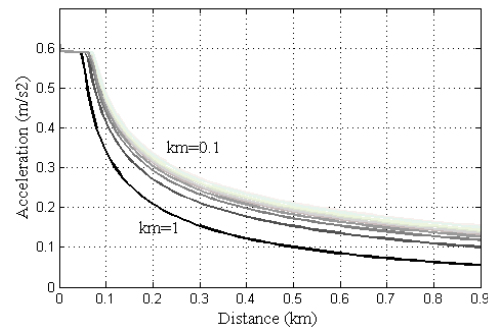

Figure 3. Acceleration curves derived from various k_m in motoring mode condition
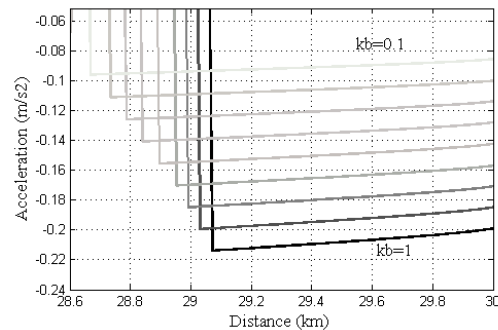

Figure 4. Acceleration curves derived from various k_b in braking mode condition

As a case study, a voyager type train [13] with parameters that are presented in Table 1 is used. The track length is assumed to be 30 km with profile, speed limit, tunnels and curvatures that are depicted in Figures 5&6.

3.1. NSGA-II Implementation

Non-dominated sorting genetic algorithm (NSGA-II) is a multi-objective optimization method introduced by Deb et al. [21]. A particular property of this algorithm is the improved computational complexity in

comparison to its predecessors that is of the order of $O(MN^2)$, where M is the number of objectives and N is the size of the population.

Table 1. Voyager train parameters

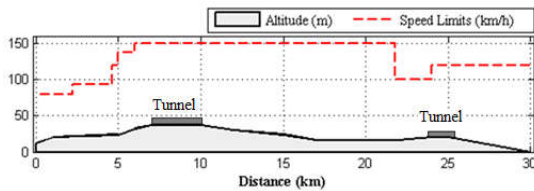|	
The maximum TE (kN)	146.8
The maximum power (kW)	1568
Mass (tones)	213.19
A	3.73
B	0.0829
C	0.0043

Figure 5. The altitude profile and location of tunnels for the selected rail path
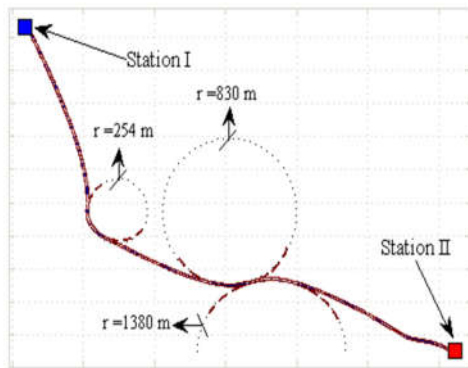

Figure 6. Curvatures of the selected rail path

Another measure in selecting this algorithm is the simplicity in implementation, and thus of its application and adaptation. This method is analogous to the ordinary genetic algorithm but with two additional functions: non-dominated sorting and crowding distance. The algorithm starts with an initial population and then with evaluating the fitness amounts, it goes to the non-dominated sorting step, Figure 7. During non-dominated sorting, every individual is ranked according to its domination rate and then it allocates to a group or a front of the space. Crowding distance is a control parameter that is calculated for each member of each front. This parameter indicates a degree of closeness of each individual to the other members in a group, as is presented in Equation (26).
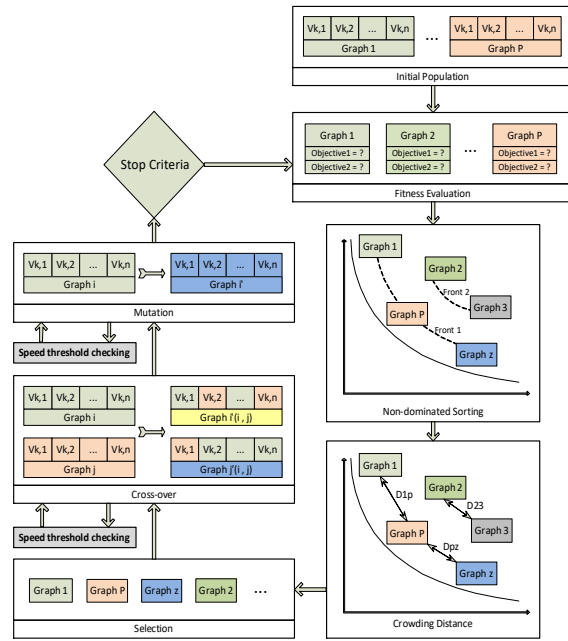

Figure 7. NSGA-II flowchart

$$D_j(k) = \sum_{i=1}^{p} \frac{f_i(k-1) - f_i(k+1)}{f_i^{\max} - f_i^{\min}} \quad (26)$$

where k is the member number existing in the jth group and i represents the objective function for a problem with p objective functions. After that, an elitist selection procedure is performed to select the best individuals for entering to the cross-over and mutation pools. During cross-over, every offspring is produced from combining two parents. For this purpose, the present research uses the simulated binary cross-over (SBC) method, which is formulated as in Equations (27) to (29):

$$\beta_{qi} = \begin{cases} (2u_i)^{\frac{1}{\eta_C + 1}} & , \ u_i \le 0.5 \\ \\ \left(\frac{1}{2(1-u_i)}\right)^{\frac{1}{\eta_C + 1}} & , \ otherwise \end{cases} \quad (27)$$

$$x_i^{[1,t+1]} = 0.5\left[(1+\beta_{qi})x_i^{(1,t)} + (1-\beta_{qi})x_i^{(2,t)}\right] \quad (28)$$

$$x_i^{[2,t+1]} = 0.5\left[(1-\beta_{qi})x_i^{(1,t)} + (1+\beta_{qi})x_i^{(2,t)}\right] \quad (29)$$

where β_{qi} is derived from the probability distribution curve η_C with random $u_i \in (0,1)$. Then two offspring are created from Equations (28) and (29). For the mutation, according to Equation (30), a probability distribution curve η_m is used that generates δ_i from a random input

$r_i \in (0,1)$. Finally, a new offspring y_i can be produced by using Equation (31).

$$\delta_i = \begin{cases} (2r_i)^{\frac{1}{(\eta_m+1)}} - 1 & , \ if \ \ r_i < 0.5 \\ 1 - [2(1-r_i)]^{\frac{1}{(\eta_m+1)}} & , \ if \ \ r_i \geq 0.5 \end{cases} \quad (30)$$

$$y_i^{(1,t+1)} = x_i^b + (x_i^b - x_i^w) \cdot \delta_i \quad (31)$$

Following up the configuration that is presented in Figure 7 an additional block named the speed threshold checking near both genetic operators is used that works as following:

By supposing a known current speed v_i in the current zone z_i, to determine a feasible speed area for the next zone, the train is moved to the next zone dynamically for two times, first with the maximum traction force and second with the minimum traction force. Thus, the accessible speed area of the next zone is determined as:

$$v_{i+1}^{acc} \in [v_{i+1_{min}}^{acc}, v_{i+1_{max}}^{acc}] \quad (32)$$

This process should be performed for all zones. Accordingly, for each genetic operator whether cross-over or mutation, if one variable of an offspring remained outside of the determined speed interval for each zone, this variable is rejected from the process and its value must be modified. It should be noted that, the optimization algorithm has infinite options to select the target speed from accessible speed area in each zone. By implementing this approach in the optimization algorithm construction, in addition to holding the continuity of the speed variables, the searching process will be guided appropriately. Although the computer processor takes more time to run the algorithm, the resulted solutions will be impressive. The above process is iterated alternatively to confirm the corresponding stop criteria.

3.2. MOPSO Implementation

Coello et al. [22] developed a multi-objective particle swarm optimization (MOPSO) algorithm for the first time. Selecting this algorithm somehow means reduced elitism when compared with NSGA-II. However, it reaches to solutions where the latter method is not capable off. The fundamental procedure of this algorithm is similar with the conventional PSO algorithm but with some additional features to generalize it to solve for multi-objective problems. A general rule always exists for all PSO-based algorithms that, each particle tries to achieve the best experience with using their personal information i.e. position and velocity. Thus, the particles select their best directions and make a movement hoping to catch better experiences. As other evolutionary strategies, the process starts with some initial particles, which here are the graph types. Then, an archive is created and absorbed all non-dominated solutions. Updating velocity and position of every particle are performed according to Equations (33) & (34).

$$V_i^{t+1} = wV_i^t + C_1 r_1(p_{best_i} - X_i^t) + C_2 r_2(g_{best} - X_i^t) \quad (33)$$

$$X_i^{t+1} = X_i^t + V_i^{t+1} \quad (34)$$

where v_i^{t+1} and x_i^{t+1} are the velocity and position of the particle i in the new iteration. V_i^t and X_i^t are the current velocity and position of the ith particle. p_{best_i} is the better position that is experienced by the ith particle. g_{best} is the best position that is experienced by the best particle. $r_1, r_2 \in (0,1)$ are random values and C_1, C_2 are cognitive and social parameters respectively.

It actually seems as a straightforward procedure but for single objective problems. Whenever, it comes to solve multi-objective problems, the algorithm seems to be complicated as is presented in Figure 8.
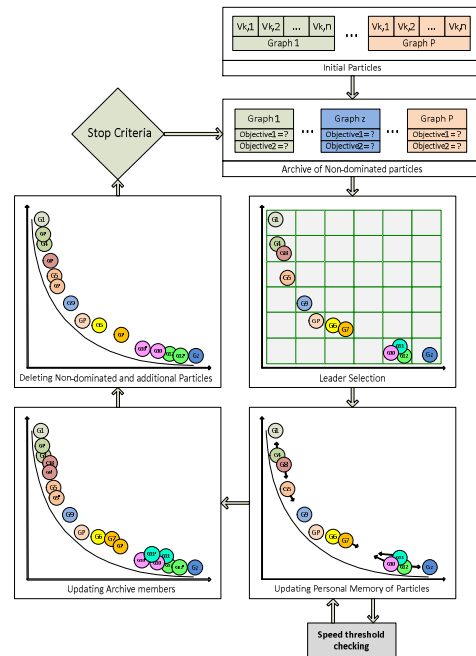

Figure 8. MOPSO flowchart

Based on the configuration in Figure 8 and in order to keep on the diversity of the solutions throughout the Pareto front optimization, a table is used to simplify selecting the leader of every particle in a multi-dimension space. It is preferred that, the leaders be selected from the boxes with minimum particles to distribute new particles appropriately throughout the front. The following expression for the Boltzmann method is used for selecting the leader.

$$p_i \quad \propto \quad \exp(-\beta n_i) \tag{35}$$

where p_i is the probability of selecting box n_i, β is the selecting effort and always $\beta > 0$. Finally the amount of p_i is concluded as in Equation (36):

$$p_i = \frac{\exp(-\beta n_i)}{\sum_j \exp(-\beta n_j)} \tag{36}$$

For the next step, the new particles with new positions and velocities are generated. Now the archive members should be updated. Dominated and additional particles will be removed from the archive at this step and they will be ready for next iteration. The speed threshold checking box is used as similar to NSGA-II for this algorithm. It means that, if a particle does not hold its variables among the determined intervals, that particle will be rejected from the process and its variables will be modified. This procedure is iterated alternatively until the stop criterion is verified and the best solutions are perfectly achieved.

4. Pareto Front

Figure 9 presents the results from the Pareto front optimization method corresponding to the NSGA-II for various members and iterations. It is obvious that, the distributed population on the Pareto front is in a convex form and also possesses a desirable diversity because of covering overall Pareto front. Solutions in the central area of the Pareto front conclude the best convergence in comparison to the other marginal solutions. The results that are obtained from 150 members and 150 iterations are more favorable than the one with 100 iterations and 100 members. In fact, the favorable diversity of the Pareto front results that are generated by the modified NSGA-II is the main reason in using this algorithm.
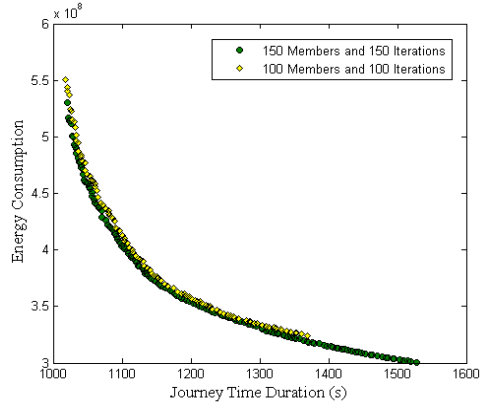

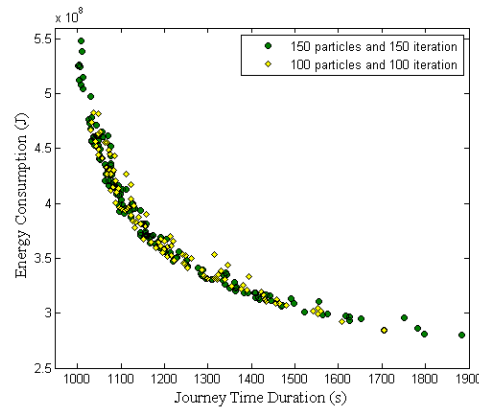Figure 9. Pareto front optimization output from NSGA-II method

Figure 10. Pareto front optimization output from MOPSO method

The two sets of the optimization results that are produced by using the Pareto front method (MOPSO) with different number of particles and iterations are presented in Figure 10. The results converge to a special front but with a poor diversity in comparison with NSGA-II. In order to compare the results that are generated by NSGA-II and MOPSO, all fronts are presented in a single plot in Figure 11. Obviously, in the marginal areas of Pareto front i.e. solutions with journey time shorter than 1100 seconds and longer than 1500 second, MOPSO can be more efficient. Moreover, in the central areas of Pareto front, NSGA-II has a favorable performance.

It should be noted that, each member in the Pareto front represents a strategy including total information required to move a train from an origin to a final destination. Thus, when a supervisor selects the final solution, the corresponding speed variables in the decision space will be distributed in the predefined zones and then the train moves to the target speeds with

an efficient driving strategy by applying suitable control sequences that were mentioned earlier.

In the present research, robustness of the optimal solutions that are provided from optimization algorithms can be assessed by applying a known perturbation to the decision space variables and then calculating the variances in the objective space by using Equation (37). If the objective space variances were limited, it can be noted that, the corresponding solution would be robust due to an identical perturbation [23]. If $f^p(x)$ is the perturbed objective function and η is the maximum variance between the main objective function $f(x)$ and the perturbed one then the robustness of solution can be expressed as in Equation (37):
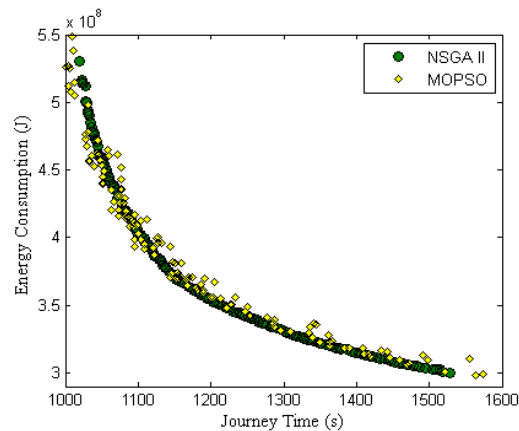

Figure 11. The Pareto fronts resulted from NSGA-II and MOPSO methods

$$\begin{cases} Minimize \; f(x) = (f_1(x), f_2(x),...,f_N(x)) \; and \; X \in S \qquad (37) \\ \\ subject \; to \quad \dfrac{\left\| f^p(x) - f(x) \right\|}{\left\| f(x) \right\|} \le \eta \end{cases}$$

4.1. Optimal Speed Trajectories

In this section, in order to compare the speed trajectories that are resulted from the two optimization algorithms, a base journey time equal to 1200 seconds is considered. The optimal speed trajectories, distance-time and acceleration profiles due to the 1200 seconds journey time determined from NSGA-II, and MOPSO are presented in Figures 12 and 13. From these results it can be observed that the braking procedures are properly acted for either stopping at the station or reaching to the lower speed levels. The acceleration curves reveal that the passenger comfort is remarkably satisfied. The position profiles demonstrate the precise

stop point of the train at the station. During the speed declining to the target lower speed level, the coasting mode is used as far as possible. However, if the train speed fails to reach its target during the critical distance, then the braking mode is used.
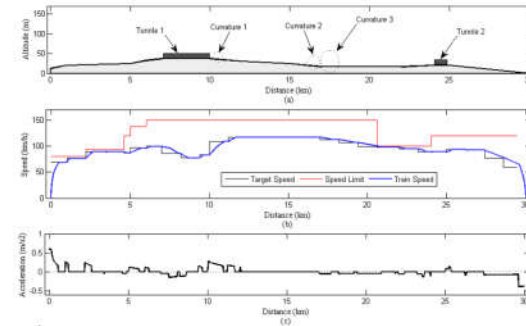

Figure 12. Speed, position and acceleration profiles obtained from NSGA-II method
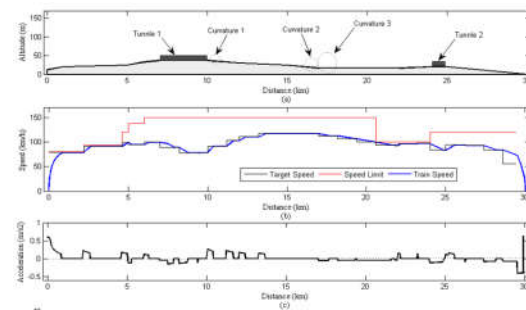

Figure 13. Speed, position and acceleration profiles obtained from MOPSO method

To stop at the station, the coasting mode is preferred before the train goes into the braking mode. Usually, in places on the track with higher resistances like the tunnels and curves, which an additional negative force is imposed on the train, the train has to consume more energy to hold its speed level. Under theses conditions, the optimal approach in terms of energy consumption would be using the coasting mode and then compensating the speed level at places of lower track resistances. The results in Figures 12&13 demonstrate that the coasting strategy is completely identified when the train goes to a situation with high resistance. In this case the tunnel is in a distance of 7 to 10 km from the station number one. The existing smoothness in the speed trajectory can be regarded as an important factor to provide for the traveler comfort during the journey. Acceleration profiles also can prove the above claim. The limited variations in the acceleration profile concludes a favorable journey in respect of the

Table 2. Summary results for three journeys at: 1040, 1200 and 1520 Seconds

Method	Journey Time (s)	Consumed Energy (J)	Robustness		Running Time (s)
			$p = 1\%$	$p = 2\%$	
NSGA-II	1040	4.756×10^8	99.47%	94.19%	24500
	1200	3.547×10^8	99.07%	96.38%	
	1520	3.012×10^8	99.67%	98.44%	
MOPSO	1040	4.531×10^8	98.48%	96.91%	21598
	1200	3.561×10^8	99.31%	98.58%	
	1520	3.013×10^8	99.69%	98.43%	

traveler comfort criteria. The energy consumption and robustness of three travels with journey time equal to 1040, 1200 and 1520 seconds that are determined from NSGA-II and MOPSO methods are presented in Table 2. In a journey time of 1040 seconds the energy consumption prediction by MOPSO is lower than NSGA-II. However, for other cases the prediction for the energy consumption by the NSGA-II method is better.

Two perturbations of 1% and 2% are used for robustness evaluations. It is observed that MOPSO solutions are more robust when compared with NSGA-II. The running time for the optimization is fairly long that is due to the complicated algorithm that is used. However, since the outcome is for achieving to an optimal ATO configuration and the desired train control system the long running time for the optimizations is not counted as a weakness in the procedures.

5. Conclusions

Applying analytical strategies to solve a multi-objective optimization problem can be sophisticated especially when the objectives are in conflict. Numerical methods such as evolutionary algorithms play a significant role in this area. In this article an optimization problem with two simultaneous and conflict objectives i.e. energy consumption and journey time delay were considered for a train to determine the optimal speed trajectories with efficient traveler comfort. To serve the purpose, two modified multi-objective optimization algorithms including NSGA-II and MOPSO were adopted. The results demonstrate that all predictions with the Pareto front optimizations converge to a unique front. It is proved that almost all feasible

solutions are attained. For a journey at 1200 seconds with near zero time delay, NSGA-II reveals a better performance when compared with MOPSO. On the other hand, the solutions that are resulted from NSGA-II prove lower robustness when a 2% perturbation from the decision space variables is used. For a journey time of shorter than 1100 seconds and longer than 1500 (i.e. solutions in marginal area of the Pareto front), MOPSO method proves a potential to generate better solutions. The resultant speed trajectories reveal that almost all the properties of an efficient journey are well identified. Through the use of the methods that are proposed in this research simultaneous improving in the energy consumption and service quality are achieved. When applied to the example railway transportation a minimized journey time delay and an increased traveler comfort are accomplished. These results can be effectively used for improving ATO and other driver assistant systems within the train configuration.

References

[1] R. Persson, E. Andersson, S. Stichel, A. Orvnäs, Bogies towards higher speed on existing tracks, International Journal Of Rail Transportation, Vol. 2, Issue 1, (2014).

[2] M. Schneider, N. Nießen, Minimising economic losses due to inefficient rescheduling, Journal of Rail Transport Planning & Management, Vol. 6, No.2, (2016), pp. 128-140.

[3] A. Fernandez-Rodriguez, A. Fernandez-Cardador, AP. Cucala, Design of robust and energy-efficient ATO speed profiles of metropolitan lines considering train load variations and delays, IEEE Transaction of

Intelligent Transportation System, Vol. 16, No. 4, (2015), pp. 2061–2071.

[4] L. Yang, K. Li, Z. Gao, X. Li, Optimizing trains movement on a railway network, Omega the International Journal of Management Science, Vol. 40, (2012), pp. 619-633.

[5] S. Lu, S. Hillmansen, C. Roberts, A power management strategy for multiple unit railroad vehicles, IEEE Transactions on Vehicular Technology, Vol. 60, (2011), pp. 406-420.

[6] K.K. Wong, T.K. Ho, Coasting control of train operation by genetic algorithm, Department of Electrical Engineering, Hong Kong Polytechnic University, Kowloon, Hong Kong, (2001).

[7] A. Moon-Ho Kang , GA-based algorithm for creating an energy-optimum train speed trajectory, Journal of International Council on Electrical Engineering, Vol. 1, No. 2, (2011), pp. 123-128.

[8] D. Yong, L. Haidong, B. Yun, Z. Fangming, A two-level optimization model and algorithm for energy-efficient urban train operation, Journal of Transportation Systems Engineering and Information Technology, Vol. 11, (2011), pp. 96-101.

[9] R. Liu, L.M. Golovitcher, Energy-efficient operation of rail vehicles Transportation Research Part A: Policy and Practice, Vol. 37, No. 10, (2003), pp. 917–932.

[10] M.H. Bigharaz, A. Afshar, A. Suratgar, F. Safaei, Simultaneous optimization of energy consumption and train performances in electric railway systems, 19th World Congress of the International Federation of Automatic Control (IFAC), Cape Town, South Africa, Vol. 47(3), (2014), pp. 6270-6275.

[11] Sh. Lu, S. Hillmansen, T. Kin Ho, C. Roberts, Single train trajectory optimization, IEEE Transactions on Intelligent Transportation Systems, Vol. 14, (2013), pp. 743-750.

[12] W. Qing, C. Cole, T. McSweeney, Applications of particle swarm optimization in the railway domain, International Journal of Rail Transportation, International Journal of Rail Transportation, Vol. 4, No. 3, (2016).

[13] R. Abousleiman, O. Rawashdeh, Electric vehicle modelling and energy-efficient routing using particle swarm optimisation, IET

Intelligent Transport Systems, Vol. 10, Issue 2, (2016), pp. 65–72.

[14] M.H. Bigharaz, Simultaneous optimization of energy consumption and service quality in electric railways, The 5th International Conference on Recent Advances in Railway Engineering, Tehran, Iran, (2003), https://www.civilica.com/Paper-ICRARE05 ICRARE05_118.html

[15] C.J. Goodman, Modelling and simulation, railway electrification infrastructure and systems, (2011), pp. 22-31.

[16] Sh. Lu, Optimising power management strategies for railway traction systems, Phd Thesis, University of Birmingham, (2011).

[17] K.K. Wong, T.K. Ho, Coast control for mass rapid transit railways with searching methods, IEE Proceedings -Electric Power Applications, Vol. 151, No. 3, (2004), pp. 365–376.

[18] S. Hillmansen, C. Roberts, Energy storage devices in hybrid railway vehicles: A kinematic analysis, Proceedings of the Institution of Mechanical Engineers, Part F: Journal of Rail and Rapid Transit, Vol. 221, No. 1, (2007), pp. 135–143.

[19] R. Chevrier, G. Marlière, J. Rodriguez, Saving energy in railway management with an evolutionary algorithm, 9th World Congress on Railway Research, Lille, France; (2011).

[20] B.P. Rochard, F. Schmid, A review of methods to measure and calculate train resistances, Proceedings of the Institution of Mechanical Engineers, Part F: Journal of Rail and Rapid Transit, Vol. 214, No. 4, (2000), pp. 185–199.

[21] K. Deb, A. Pratap, S. Agarwal, T. Meyarivan, A fast and elitist multiobjective genetic algorithm: NSGA-II, IEEE Trans. on Evolutionary Computation, Vol. 6, No. 2, (2002), pp. 182-197.

[22] C.A.C Coello, G.T. Pulido, M.S. Lechuga, Handling multiple objectives with particle swarm optimization, IEEE Trans. on Evolutionary Computation, Vol. 8, No. 3, (2004), pp. 256-279.

[23] J. Andersson, Multiobjective optimization in engineering design, Phd Thesis, Department of Mechanical Engineering Linköpings University, Sweden, (2001).